Journal of Theoretical Biology 262 (2010) 346–360

Contents lists available at ScienceDirect

Journal of Theoretical Biology

journal homepage: www.elsevier.com/locate/yjtbi

Towards a correct description of zooplankton feeding in models: Taking into account food-mediated unsynchronized vertical migration

A.Yu. Morozov [a,b,*], E.G. Arashkevich [b]

[a] Department of Mathematics, University of Leicester, Leicester LE1 7RH, UK
[b] Shirshov Institute of Oceanology, 36 Nakhimovskiy, Prospekt, RAS, 117997 Moscow, Russia

ARTICLE INFO

Article history:
Received 30 June 2009
Received in revised form
30 August 2009
Accepted 16 September 2009
Available online 24 September 2009

Keywords:
Non-synchronous vertical migration
Functional response
Grazing control
Vertical distribution

ABSTRACT

Complex nature of foraging behaviour of zooplankton makes it difficult to describe adequately zooplankton grazing in models with vertical space. In mean-field models (based on systems of PDEs or coupled ODEs), zooplankton feeding at a given depth is normally computed as the product of the local functional response and the zooplankton density at this depth. Such simplification is often at odds with field observations which show the absence of clear relationship between intake rates of organisms and the ambient food density. The observed discrepancy is generic and is often caused by fast non-synchronous vertical migration of organisms with different nutrition status. In this paper, we suggest a simple way of incorporating unsynchronized short-term vertical migration of zooplankton into the mean-field modelling framework. We compute grazing of zooplankton in each layer depending on feeding activity of organisms in the layer. We take into account grazing impact of animals which are in the active phase of foraging cycle at the given moment of time but neglect the impact of animals which are in the non-active phase of the cycle (e.g. digesting food). Unsynchronized vertical migration determines the vertical distribution of actively feeding animals in layers depending on vertical distribution of food. In this paper, we compare two generic plankton models: (i) a model based on 'classical' grazing approach and (ii) a model incorporating food-mediated unsynchronized vertical migration of zooplankton. We show that including unsynchronized food-mediated migration would make the behaviour of a plankton model more realistic. This would imply a significant enhancement of ecosystem's stability and some additional mechanisms of regulation of algal blooms. In the system with food-mediated unsynchronized vertical migration, the control of phytoplankton by herbivorous becomes possible even for very large concentrations of nutrients in the water (formally, when the system's carrying capacity tends to infinity).

1. Introduction

Adequate description of zooplankton feeding is of vital importance for construction of plankton models with high predictive power. A major difficulty in modelling arises due to the fact that zooplankters usually perform active movement along vertical direction and adjust their location to maximize their fitness (McLaren, 1963; Han and Straskraba, 1998) or/and to minimize the risk of being eaten (Bollens and Frost, 1989; Lampert, 1992). Note that those processes are related to complex foraging strategies of organisms and it is difficult to describe them via a simple diffusion–advection scheme (Iwasa, 1982; Leising et al., 2005). In this paper, we will be mostly concerned with modelling of feeding of herbivorous zooplankton.

Foraging behaviour of herbivorous includes processes taking place at different time and space scales. The feeding cycle with the largest time and space scales is the well-known regular diel vertical migration, when herbivorous ascend to the surface layers at night for feeding and descend to deep layers during day time. Such strategy helps avoid visual predators in the surface layer (Bollens and Frost, 1989; Ohman, 1990; Lampert, 1992). Foraging behaviour of zooplankton manifests itself also at intermediate time and space scales (1–3 h and dozens of metres). An important example is short-term exchanges during the night feeding between high food surface layers, where organisms graze, and deeper layers, where organisms digest the consumed food (Leising et al., 2005 and the references therein). Finally, herbivorous shows rather complex behaviour at microscales of several centimetres and seconds which has been well studied and documented (Tiselius and Jonsson, 1990; Malkiel et al., 2003).

In mean-field plankton models (based on PDEs or coupled ODEs) with explicit vertical resolution, consumption of food by zooplankton is described based on the following concept. The

* Corresponding author at: Department of Mathematics, University of Leicester, Leicester LE1 7RH, UK.
E-mail address: am379@le.ac.uk (A.Yu. Morozov).

0022-5193/$ - see front matter © 2009 Elsevier Ltd. All rights reserved.
doi:10.1016/j.jtbi.2009.09.023

grazing rate at a given depth is computed by $f(P)Z$, i.e. by the product of the local functional response $f(P)$ and zooplankton density Z at this depth. The local functional response is understood as the specific food intake rate (i.e. per biomass of a zooplankter per unit of time) as a function of the ambient food density (Jeschke et al., 2002; Gentleman et al., 2003). Functional responses of herbivorous are normally measured in laboratories by estimating ingestion rates of organisms for different initial amounts of food (e.g. DeMott, 1982; Hansen et al., 1990).

We should say, however, that implementation of the above concept in modelling can be rather erroneous and misleading despite its wide adaptation in the literature. The point is that it often becomes at odds with field observations. Indeed, if we plot ingestion rates (or gut contents) of grazers measured *in situ* versus the ambient food density, the resulting graph usually resembles a 'cloud' of points without any clear relationship (e.g. Boyd et al., 1980; Dagg and Wyman, 1983; Tseng et al., 2008). In Section 2, we provide a typical example of such situation based on our own data on copepods' feeding in the ocean. It is impossible to fit satisfactorily the observed data with any of the existing types of functional responses. Only positive correlation between consumption rates and the amount of ambient food can be detected (Boyd et al., 1980).

Interestingly enough, the absence of clear relationship between ingestion rates and the ambient food density in the real ocean is not a consequence of a strong environmental noise only. The point is that a large number of specimens simply do not graze at depths where they dwell most of time. They move to those depths either to digest the food that they have grazed or to escape from predators or due to some other reasons (Dagg and Wyman, 1983; Cottier et al., 2006). Thus the observed non-existence of local functional response is presumably a consequence of complex foraging behaviour of zooplankton at intermediate time and space scales and not a result of noise. Note that this phenomenon is rather different from the daily-based vertical migration pattern since it implies an exchange of organisms between different layers in a unsynchronized way without a pronounced alteration of the vertical profile of zooplankton (Leising et al., 2005; Cottier et al., 2006).

The absence of functional response due to unsynchronized vertical migration can seriously affect modelling results obtained based on the classical local grazing approach. A possible solution could be implementation of the individual based modelling (IBM), where vertical displacement and feeding of each organism is described by its own equation. However, we should say that despite its wide adaptation in plankton literature (see Carlotti and Wolf, 1998; Leising, 2001; Batchelder et al., 2002; Leising et al., 2005), the implementation of the IBM can be of limited use. This is especially true in case one is interested in generic properties of plankton systems. The point is that after having done a large number of simulations, we still do not get a clear understanding of system's dependence on model parameters, basic mechanisms of ecosystem's regulation, etc. Note also that rules governing the behaviour of individual zooplankters in the real ocean are still poorly understood, especially on intermediate time scales (Leising et al., 2005; Fossheim and Primicerio, 2008). Thus, a slight change of rules of species interaction in an IBM system might alter completely model's behaviour. Finally, the number of organisms in the water column is usually large ($>10^3$–10^4 inds./m^2), which would imply the use of large number of equations. As such, an important question is whether the well-established mean-field framework can be extended somehow to include unsynchronized feeding of zooplankton?

In this paper, we suggest a simple way of incorporating unsynchronized exchange of herbivorous between layers into the mean-field modelling framework, operating with mean population densities. While computing grazing of zooplankton, we take into account consumption of algae by those animals which are in the active phase of foraging cycle at the given moment of time and neglect the impact of those which are in the non-active phase of the cycle. The distribution of actively grazing animals among the layers becomes adjusted to that of phytoplankton via a food-mediated unsynchronized vertical migration of zooplankton. We consider two generic plankton models with an explicit space: (i) model based on the 'classical' grazing approach and (ii) model incorporating food-mediated unsynchronized vertical migration. Comparison of the two models reveals that the model with unsynchronized vertical migration exhibits more realistic behaviour that the classical one.

The paper is organized as follows. In Section 2, we show (based on our field data) that the computation of grazing as the product of the local functional response and the ambient density of zooplankton in a given layer may be erroneous and the observed discrepancy is not a result of the environmental noise but that of complex foraging behaviour of zooplankton. In Section 3, we construct a generic mean-field spatially resolved model incorporating effects of food-mediated unsynchronized vertical migration. In Section 4 we compare the constructed model with the plankton model based on the classical grazing approach. In Section 5, we discuss some advantages of taking into account food-mediated unsynchronized vertical migration in plankton models.

2. Revealing patterns of zooplankton feeding *in situ*

In this section, we show that in the real ocean, one can hardly talk about the existence of local functional response of zooplankton. In other words, there is no clear functional relationship between the feeding rate and the ambient food density at a given depth. Such situation is not a result of the influence of environmental noise only but that of complex feeding strategies of herbivorous.

The observations were carried out in the central northern Barents Sea during three cruises of R/V *Jan Mayen* in July 2003 and 2004, and May 2005. Zooplankton samples were taken twice a day (at noon and midnight) from 100–50, 50–20 and 20–0 m. The biomass, species abundance, demography and ingestion rates of the dominant copepod species *Calanus glacialis* were measured as well as the vertical distribution of food. All details on the collection of material and the methods implemented can be found in Morozov et al. (2008).

Fig. 1 represents local functional responses of *Calanus* spp. in the ocean, i.e. the ingestion rates plotted versus the ambient density of food in layers where the organisms were caught. We show the local responses only for the late copepodite stages (VI to IV). The grazing impact of younger stages was evaluated to be rather small in the overall grazing. Fig. 1A shows local responses of *Calanus glacialis* within the whole range of the observed ambient food density ($0<P<15\,\mu$g Chl a/m^3). Fig. 1B is a zoom of the same graph at food densities when the saturation in ingestion is not well pronounced ($0<P<6\,\mu$g Chl a/m^3). By triangles, we show separately the ingestion rates in the deepest layer for some reasons explained later.

From the graphs in Fig. 1, one can suggest that there exists no clear functional dependence of ingestion rates on the ambient food density, at least, at low and intermediate food densities. To make this suggestion more convincing we have completed an extensive statistical treatment of the data. The results are summarized in Table 1. We conducted the non-linear regression analysis and considered three possible types of functional response as fitting models. These are Holling types of response (Jeschke et al., 2002; Gentleman et al., 2003). To parameterize the

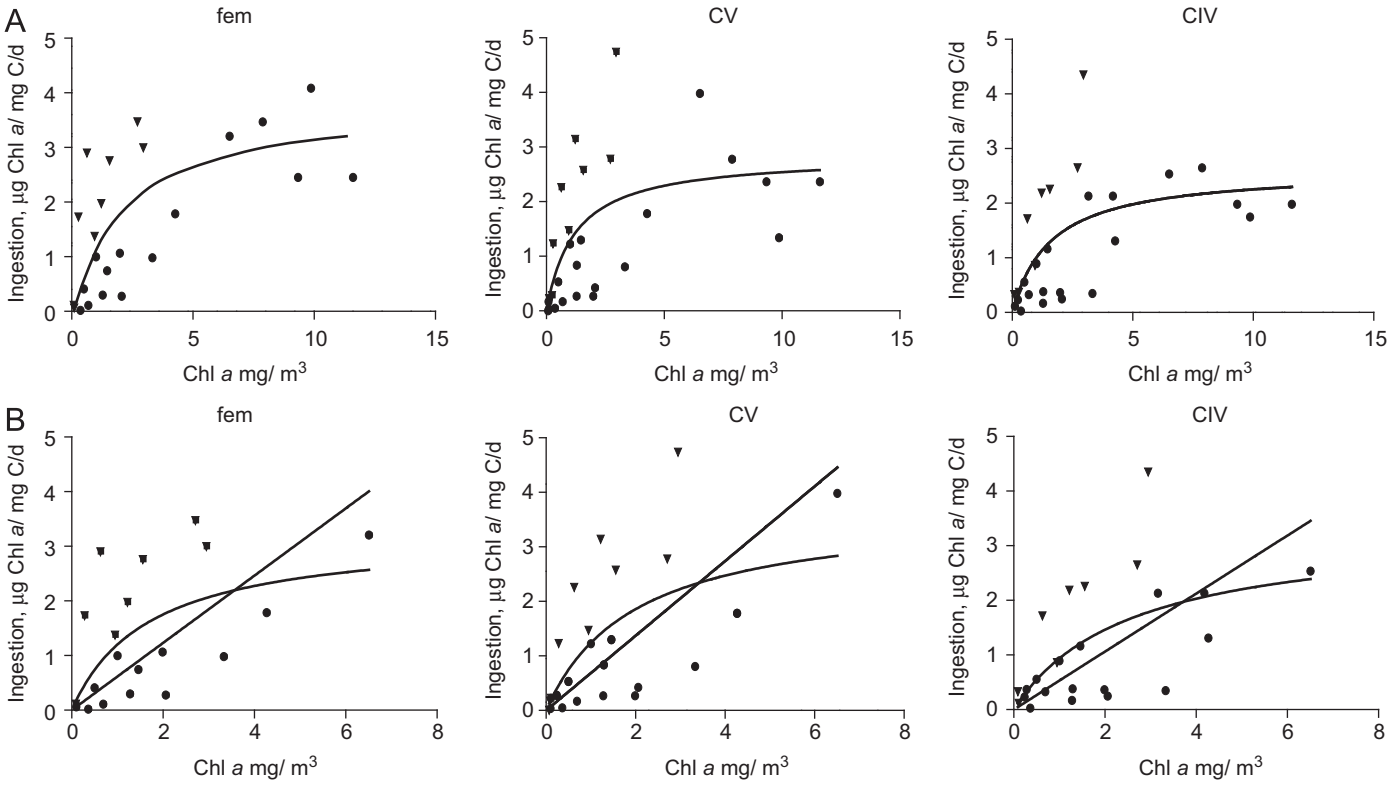

Fig. 1. Local functional responses of *Calanus* sp, measured *in situ* (the central northern Barents Sea). Ingestion rates are plotted versus the ambient food density in layers where the organisms were caught. (A) The local responses within the whole range of the observed food density. (B) Zoom of the same local responses at low and intermediate food densities, before saturation. By triangles, we show the ingestion rates in the deepest layer (50–100 m). The fitting curves are obtained by the LSM and discussed in detail in the text.

Table 1
Non-linear regression analysis of patterns of zooplankton feeding shown in Fig. 1. (A) The fitting function is Holling type II response parameterized by $\alpha P/(1+\beta P)$. (B) The fitting function is Holling type I (linear) response. Statistical treatment is fulfilled for low and intermediate food densities.

Copepod stage and the range of food density (mg Chl/m^3)	Best-fit for a: $\alpha P/(1+\beta P)$	Best-fit for b: $\alpha P/(1+\beta P)$	CI (95%) for a	CI (95%) for b	R^2
(A)					
Fem $0<P<14$	1.680	0.4513	0.2864–3.074	−0.0994–1.0023	0.4631
CV $0<P<14$	2.337	0.8201	−0.08549–4.760	−0.3297–1.9702	0.3935
CIV $0<P<14$	1.628	0.6225	0.0679–3.187	−0.2187–1.4642	0.3931
Fem $0<P<6$	1.907	0.5886	−0.4529–4.266	−0.6247–1.8022	0.2985
CV $0<P<6$	1.863	0.5035	0.2720–3.455	−0.2668–1.2741	0.3901
CIV $0<P<6$	1.304	0.3923	−0.1332–2.7420	−0.4131–1.1980	0.3496

Copepod stage and the range of food density (mg Chl/m^3)	Best-fit for a: αP	CI (95%) for a	R^2
(B)			
Fem $0<P<6$	0.6155	0.3940–0.8370	0.1282
CV $0<P<6$	0.6848	0.4967–0.8728	0.2603
CIV $0<P<6$	0.5308	0.3585–0.7031	0.2302

response we used: (i) the linear response aP (Holling type I), (ii) Holling type II response given by $aP/(1+bP)$ and (iii) the sigmoid response (Holling III type) given by $aP^2/(1+bP^2)$. We found that the best fitting within the whole range of food density is provided by Holling type II response which is presented in the table. The corresponding fitting curves are plotted in Fig. 1A. On the contrary, at low and average food densities of data set A (Fig. 1B), the linear fitting describes better feeding for stages CVI and CIV, whereas Holling type II becomes a better fit for stage CV (thus we show both fitting models).

Based on Table 1, one can conclude that more or less satisfactory fitting of the data becomes possible only when we cover the whole range of food density. This is due to a number of points corresponding to saturation in ingestion. On the contrary, fitting becomes unsatisfactory at low and intermediate food densities. This can be seen from large corridors for the confidential intervals as well as from low values of R^2. One can hardly talk about the existence of a local functional response at low and intermediate food concentrations, i.e. during non-blooming periods. We emphasize that this is the behaviour of

functional response at low and intermediate of densities which determines ecosystem's stability and possibility of grazing control in models. Another important issue is that the number of organisms corresponding to the points scattered far from the fitting curves in Fig. 1 is sufficiently large in the whole number of individuals in the column (their 'weights' are high) and we cannot neglect their impact.

We should note that the absence of local function response of herbivorous is rather typical for real ecosystems and have been reported earlier in the literature (Boyd et al., 1980; Tande and Båmstedt, 1985; Dagg and Wyman, 1983; Tseng et al., 2008). As such, some important questions arise then. What is the main cause of the observed absence of clear functional dependence of consumption rates on the ambient food density? Why cannot we get nice-looking graphs of functional responses similar to those obtained in the experimental feeding in laboratories (cf. DeMott, 1982; Hansen et al., 1990)?

An 'evident' answer would be taking into account the influence of environmental noise which is stronger in the real ocean than in laboratory aquaria. However, there is another more important issue what we need to take into consideration. This is related to complex foraging behaviour of zooplankton. The point is that organisms, caught in layers with poor nutrition conditions, often migrate to those layers for digestion or to avoid predators or for some other reasons (Dagg and Wyman, 1983; Leising et al., 2005). Such situation can be seen from Fig. 1 which reveals that high ingestion rates at low food densities are due to the grazing impact of individuals caught in the deep layer (denoted by triangles). All the triangles are situated well above ingestion rates obtained in surface layers, the food concentration being the same. In case of a strong noise, the 'triangles' would be scattered randomly on the graph which is actually not observed. The reason is that the individuals caught in the deep layer have filled their guts by grazing in upper layers. Plotting ingestion rates versus the ambient food does not make much sense in this case.

Note that by comparing night and day vertical distributions of zooplankton, we did not find any statistically significant difference between the profiles. At the same time, the gut passage time of *Calanus* spp. is approximately 1–2 h (Dagg and Walser, 1987, Arashkevich, unpublished data). As such, active vertical displacement of zooplankton was non-synchronous and involved exchanges of individuals between the layers without changing the vertical profile of zooplankton population as a whole. We call this phenomenon the unsynchronized vertical migration of zooplankton. By analysing the current data, we found some more evidence of the existence of unsynchronized vertical migration for the given species. We are going to describe this non-trivial phenomenon in more detail in our satellite paper.

There is an important consequence from the above for constructing plankton models: the classical computation of zooplankton grazing in layer i as $f(P_i)Z_i$ would be too simplistic and erroneous.

3. Mathematical model

In this section, we construct a generic model of phytoplankton dynamics with explicit vertical resolution taking into account non-synchronous foraging cycles of zooplankton. We apply an approach based on coupled ODEs. We split the whole euphotic zone into n horizontal layers. For the sake of simplicity, we consider all layers to have the same widths. In layer (i), variations of phytoplankton densities (P_i) are described by the following system of ODEs:

$$\frac{dP_i}{dt} = \tilde{r}_i P_i - f_i(P_i)\tilde{Z}_i(P_1, P_2, \ldots, P_n), \tag{1}$$

where $\tilde{r}_i$ is the phytoplankton growth rate, $f_i(P_i)$ is the functional response in layer i, $\tilde{Z}_i$ is the density of individuals which are in the active phase of their foraging cycle at the given moment of time. Note that the density $\tilde{Z}_i$ differs from the actual zooplankton density Z_i which gives the total number of specimens per unit volume (i.e. including those digesting food). The value of $\tilde{Z}_i$ depends on the distribution of food in the water column, i.e. on $\{P_i\}$, $i=1, n$. Such a way of parameterization of grazing term requires some comments.

The point is that feeding of a zooplankter is not a continuous process in time (Leising et al., 2005 and the references therein). Rather, it includes periods of consumption of food (the active phase) as well as periods of digestion and rest (the non-active phase). We consider that the zooplankton population feeding cycles are not synchronized in time. When computing consumption of phytoplankton in each layer, we should take into account only the impact of zooplankters $\tilde{Z}_i$ which are in the active phase of the cycle and not the whole density Z_i. In general, the amount $\tilde{Z}_i$ of actively grazing individuals is not proportional to the total amount Z_i of zooplankton due to unsynchronized vertical exchange of well-fed and hungry animals between the layers. Such an exchange is different for different layers and depends on the vertical distribution of food $\{P_i\}$. In other words, vertical distribution of food would determine the partition of actively grazing animals among layers. The time of change of vertical position of a zooplankter is much smaller (1–2 h) than the characteristic time of change of phytoplankton biomass in the water column (1–2 days). As such, we may consider that the vertical distribution of actively feeding zooplankton becomes quickly adjusted to relatively slow changes in the distribution of food.

The density of actively feeding zooplankton in layer i can be rewritten as

$$\tilde{Z}_i = \frac{\tilde{Z}_i}{n\tilde{Z}} \tilde{Z} n = \alpha_i \tilde{Z} n, \tag{2}$$

where $\tilde{Z} = (\tilde{Z}_1 + \cdots + \tilde{Z}_n)/n$ states for the average density of actively feeding zooplankton in the water column. The coefficient α_i describes the proportion of active feeders dwelling in layer i. The effects of unsynchronized vertical migration on grazing rate are incorporated now in terms of the consumption vector $A=\{\alpha_i\}$, which shows the distribution of active grazers over the layers. Evidently, the sum of all α_i should be equal to unity.

A further important step is parameterization of the consumption vector A. In general, the coefficients α_i are not constant and depend on the distribution of food as well as on the location of layers, i.e. on their depths. For example, all food conditions being equal, layers with deeper depths might be preferable since they provide a better refuge from predators (Fossheim and Primicerio, 2008; Daase et al., 2008). To make a further progress in understanding the model's properties, we need, however, to make some simplifications. We will consider the scenario when the coefficients α_i are equal to the relative proportion of amount of food in the layers:

$$\alpha_i = \frac{P_i}{\sum_i P_i}. \tag{3}$$

We should say that in this generic model, we are interested in the phytoplankton dynamic during rather short time periods (say, 10 days). As such, we suggest the whole zooplankton biomass to be approximately constant. Also, we shall consider that the total number of active feeders does not depend on the amount (and distribution) of food in the column, i.e. $\tilde{Z} = \theta Z_{tot}$, where Z_{tot} is the average zooplankton density, $\theta=const$ is the proportion of active feeders in the zooplankton population at each moment of time. To describe the phytoplankton growth rate we use the logistic function, i.e. $\tilde{r}_i P_i = r_i P_i(1 - P_i/K)$, where K is the carrying capacity.

We take into account attenuation of growth of phytoplankton in lower layers by the phytoplankton from upper layers and describe the self-shading via a standard way by multiplying r_i by $\exp(-\gamma(P_1+\cdots+P_{i-1})\Delta)$, where Δ is the width of a layer In other words, the light attenuation coefficient due to self-shading is proportional to the phytoplankton density (Herman and Platt, 1983).

We consider the local functional response $f_i(P_i)$ in (4) to be of Holling type II given by the hyperbolic parameterization (Holling, 1959; Gentleman et al., 2003):

$$f_i(P_i)=\frac{\omega_i P_i}{1+\beta_i P_i}. \tag{4}$$

We arrive at the following system of ODEs for the phytoplankton densities P_i:

$$\frac{dP_i}{dt}=r_i\exp\left(-\gamma_0\sum_{j=1}^{i-1}P_j\right)P_i\left(1-\frac{P_i}{K}\right)-\mu_i\frac{P_i}{1+\beta_i P_i}\frac{P_i}{P}, \tag{5}$$

where P is the average density of phytoplankton in the column, i.e. $P=(P_1+\cdots+P_n)/n$; μ_i is defined by $\mu_i=\omega_i\theta Z_{tot}$, $\gamma_0=\gamma\Delta$, Δ is the width of a layer. Note that for $i=1$ we do not have an exponential multiplier in the corresponding growth rate term.

Along with the above model accounting for unsynchronized vertical migration, we will consider briefly the 'classical' model with grazing terms obtained from (5) by assuming equal proportions of active feeders and all layers. In this case, the model equations become

$$\frac{dP_i}{dt}=r_i\exp\left(-\gamma_0\sum_{j=1}^{i-1}P_j\right)P_i\left(1-\frac{P_i}{K}\right)-\mu_i\frac{P_i}{1+\beta_i P_i}. \tag{6}$$

For both models we use $\mu g\,C\,l^{-1}$ as the unit of phytoplankton densities. The system parameters are considered to vary within the following ranges found in the literature: $0.05<r_i<21$/day (Edwards and Brindley, 1999); $50<K<100\,\mu g\,C\,l^{-1}$ (Franks, 2001); $0.01<\theta\omega_i<0.1\ 1/\mu g\,C\,l^{-1}$/day; $0.005<\beta_i<0.1\ 1/\mu g\,C\,l^{-1}$ (Hansen et al., 1990; Edwards and Brindley, 1999). Note that the $\theta\omega_i$ has the meaning of maximal of average grazing rate of a copepod during the feeding cycle. The attenuation constant γ can be estimated from Herman and Platt (1983). We consider, approximately, that the total depth of the water column is $H=100$ m. This gives us an estimate for γ: $0.05<\gamma<1\ 1/(\mu g\,C\,l^{-1}/m)$, the width of each layer is given by $\Delta=H/n$.

The ranges of the maximal grazing rates μ_i for models (5) and (6) should be estimated separately. For the model with unsynchronized migrations, μ_i is defined as $\mu_i=\omega_i\theta Z_{tot}$, where Z_{tot} is the average zooplankton density of zooplankton in the column. We will consider Z_{tot} to vary within $1<Z_{tot}<20\,\mu g\,C\,l^{-1}$, this gives $0.01<\mu_i<2$/day. In the model (6), μ_i is defined by $\mu_i=\omega_i\theta Z_i$, where Z_i is the zooplankton density in layer i, the meaning of θ is the same as before. In other words, in model (6) the proportion of actively feeding organisms in each layer is constant. Vertical distribution of the zooplankton in the column, Z_i can vary largely for a fixed value of the average density Z_{tot}. However, the difference among Z_i normally should not exceed certain limits. This is true both for systems with no diel vertical migration (e.g. Morozov et al., 2008) and systems with diel vertical migration (e.g. Ohman, 1990), in the latter case we understand Z_i as the night-day average. Here we will consider that the ratio $\max(Z_i)/\min(Z_i)$ is limited by 100 which is consistent with data on real ecosystems. This gives a rough estimate $1<\max(\mu_i)/\min(\mu_j)<100$, assuming $\omega_i=\omega$. Also we shall consider that $0.01<\max(\mu_i)<2$/day (as for model (5)).

4. Modelling results

4.1. Plankton model with the classical grazing terms

Here we consider briefly the properties of the model with grazing terms given by (6). The dynamics of this model is rather simple since the only model's attractors are stationary states (self-sustaining oscillations are impossible). The stability conditions of the stationary states are provided in Appendix A. Depending on system parameters, the model can possess a unique stable stationary state with persistence of phytoplankton in all layers ($P_i\neq 0$, $i=1,n$); otherwise, the phytoplankton would be overgrazed and go extinct, at least, in one layer. Our comprehensive investigation shows, however, that persistence of phytoplankton is hardly possible within a realistic parameter range. Note that the model depends on a large number of parameters (e.g. for $n=3$, there are 11 parameters in total) and it is rather hard to visualize the model's parametric portrait in such highly dimensional space. We use the following method to have an insight into the structure of the system's parameter space.

Let us consider the number of layers $n=3$, this gives $0.08<\gamma_0<1.6$. We assume the half-saturation constants to be the same in each layer $\beta_1=\beta_2=\beta_3=\beta$. Also, we suggest that the growth rates of phytoplankton in different layers are related as $r_2=\lambda r_1$; $r_3=\lambda r_2$, ($\lambda\leq 1$). For each set of parameters we consider that the maximal grazing rates μ_i in the layers cannot differ from each other by several orders of magnitude (see some comments at the end of the previous section). In particular, we suggest that for a given μ_1 in the surface layer, the other coefficients μ_i ($i=2,3$) vary within some range $\mu_1/\varepsilon\leq\mu_{2,3}\leq\varepsilon\mu_1$, where $100>\varepsilon>1$.

Fig. 2 shows the location of the persistence domain in the parameter space. The diagram was constructed by verifying conditions (A7–A12) of existence of a stable stationary state from Appendix A for a given point in 6-D parameter space (γ_0, K, r, μ_1, μ_2, μ_3). We fixed the two first parameters and considered different possible combinations of the other four parameters taking into account the above condition on μ_i for different fixed values of ε. The ranges of all system's parameters are given in the end of Section 3.

Fig. 2A represents persistence domain in (γ_0, K) plane, showing the key role of light attenuation and the carrying capacity. Persistence is possible for the parameters lying below one of the curvilinear boundaries (curves 1–4), which are constructed for different ε, providing different corridors for the maximal grazing rates. For each (γ_0, K), belonging to the persistence domain, there exist r, μ_1, μ_2, μ_3 such that model (6) possesses a non-trivial stationary stable state. For parameters situated above the boundary, this is impossible for any r, μ_1, μ_2, μ_3. The hatched region corresponds to biologically feasible γ_0, K. One can see that for the equal maximal grazing rates in the layers ($\varepsilon=1$), the model always predicts an extinction phytoplankton at least, in one layer. Persistence becomes possible only in a rather small portion of the hatched region only when the maximal grazing rates μ_i show a pronounced difference. Note, however, that even in this case, persistence is rather questionable from a biological point of view.

The latter statement is illustrated by Fig. 2B, C. Fig. 2B shows persistence domain in (r,μ_1) plane for the fixed $K=55$, $\gamma_0=0.09$, $\varepsilon=100$. For (r,μ_1) belonging to the persistence domain in Fig. 2B there exist some (μ_2,μ_3) which provide a non-trivial stable stationary state. The existence of such a state was verified based on (A7–A12) by considering possible combinations of (μ_2,μ_3). First, one can see from the figure that such domain is rather small in size. Second, Fig. 2C shows the persistence domain in (μ_2,μ_3) for fixed $r=1$, $\mu_1=0.8$, $K=55$, $\gamma_0=0.09$ (i.e. for a fixed point in persistence domain in (r, μ_1) plane). From Fig. 2C one can see that persistence of phytoplankton takes place for rather small values of μ_2, μ_3 compared to μ_1. Biologically, smallness of μ_2, μ_3

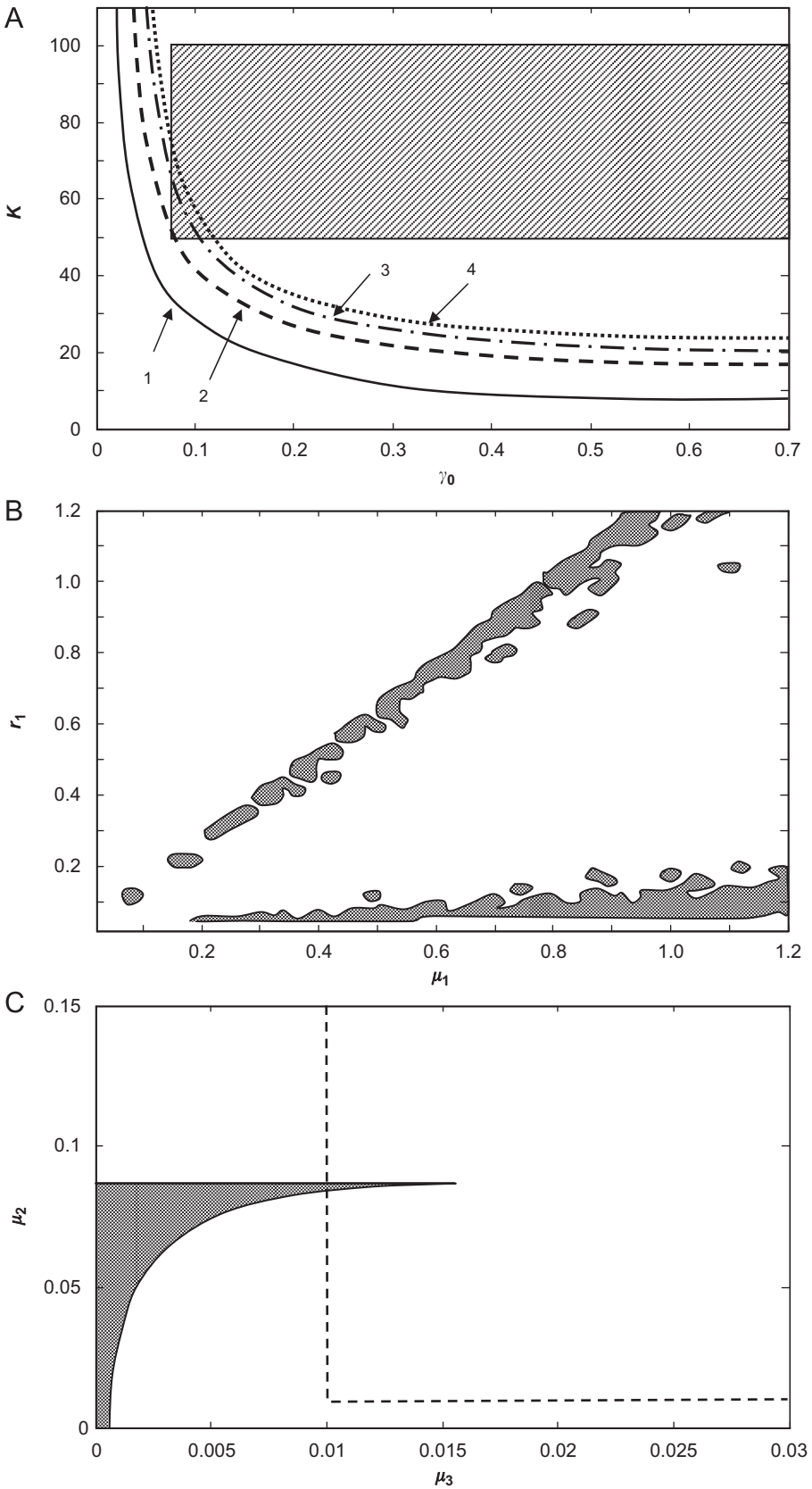

Fig. 2. Persistence domains in the parameter space of model (6). For details see text. (A) Persistence domain in (γ_0, K) plane. The hatched region corresponds to biologically feasible γ_0, K. Persistence is possible for the parameters lying below one of the curvilinear boundaries (curves 1–4), constructed for different ε, where $\varepsilon=\max(\mu_i)/\min(\mu_j)$. Here $\varepsilon_1=1$; $\varepsilon_2=10$; $\varepsilon_3=50$; $\varepsilon_4=100$. (B) Persistence domain (hatched) in (r,μ_1) plane constructed for $K=55$, $\gamma_0=0.09$, $\varepsilon=100$. (C) Persistence domain (hatched) in (μ_2,μ_3) plane constructed for $r=1$, $\mu_1=0.8$, $K=55$, $\gamma_0=0.09$, $\varepsilon=100$. Dotted lines show the lowest possible limits of μ_2, μ_3.

may be justified only by a pronounced decrease in the amount of zooplankton in deep layers i=2, 3. On the other hand, computing of P_i shows that algal densities in all layers are close to each other. This signifies that persistence would require avoidance by zooplankton of deep layers with similar nutrition conditions as those at the surface layer. This is not typical for real plankton communities and seems to be an artefact of model (6). Note that the graphs plotted in Fig. 2 are shown for the equal growth rates coefficients (i.e. λ=1). Considering a more realistic situation ($\lambda < 1$) with makes the persistence even less possible (persistence domains shrink). Also, considering different number of horizontal layers n would result in similar conclusions.

To complete a brief enumeration of drawbacks of model (6), we should mention that the persistence of phytoplankton in the water column becomes impossible with an increase of the carrying capacity K (see Fig. 2A), other parameters being fixed. The only regime becomes the one characterized by a high density of phytoplankton in the upper layer (close to the carrying capacity K) and zero densities in all other layers due to overgrazing. This is, definitely, at odds with the reality which shows that even in highly eutrophic systems there algae can persist in the whole water column.

4.2. Plankton model with food-mediated unsynchronized vertical migration

The mentioned above difficulties disappear when we incorporate into model (6) food-mediated unsynchronized vertical migration. In this paper, we consider model (5) when the number of layers n=3 (the case of $n \neq 3$ is briefly addressed at the end of this section). We should say that analytical treatment of this model becomes rather complicated compared to (6). Even determining the number of non-trivial stationary states requires numerical simulations.

Model (5) is discontinuous at zero. However, we can define the right-hand side functions to be zeros at this point; thus, the origin becomes a stationary state of the system. The zero stationary state signifies extinction of phytoplankton in all layers. This state is stable (locally) when the following inequality holds (see Appendix B):

$$r_1\mu_2\mu_3 + r_2\mu_1\mu_3 + r_3\mu_1\mu_2 - 3\mu_1\mu_2\mu_3 < 0. \quad (7)$$

For the opposite sign of (7), the zero state becomes unstable and persistence of algae in all layers is guaranteed (we consider that all initial P_i are larger than zero). In Appendix C we prove analytically that the loss of stability of the trivial stationary state occurs via a birth of a stable stationary state in the vicinity of zero.

Let us consider first that the attenuation of light in the water is mostly due to self-shading by algae and suggest also that the local functional responses in all layers are the same. This signifies that $r_i = r$, $\omega_i = \omega$, $\beta_i = \beta$, $\mu_i = \mu$. The condition of persistence of phytoplankton (7) becomes $r > \mu$. Further, we shall address briefly the cases when $r_1 > r_2 > r_3$ (strong absorption of light by water) and when the local functional responses are different.

By conducting extensive numerical simulations we found that there are three different types of system's behaviour related to the number and position of the stable stationary states ($r > \mu$). The corresponding phase portraits are shown in Fig. 3 (obtained for different β, the other parameters being the same). Fig. 3A shows the persistence of phytoplankton in all layers at low densities in a non-blooming regime ($P_i \ll K$). This is observed at low β, i.e. for high values of saturation of food consumption. For somewhat larger β, the system might exhibit bistability (Fig. 3B). In this case, starting from different initial conditions, the trajectories are attracted by different stable states: one characterized by low algal densities in all layers (the non-blooming regime) and the

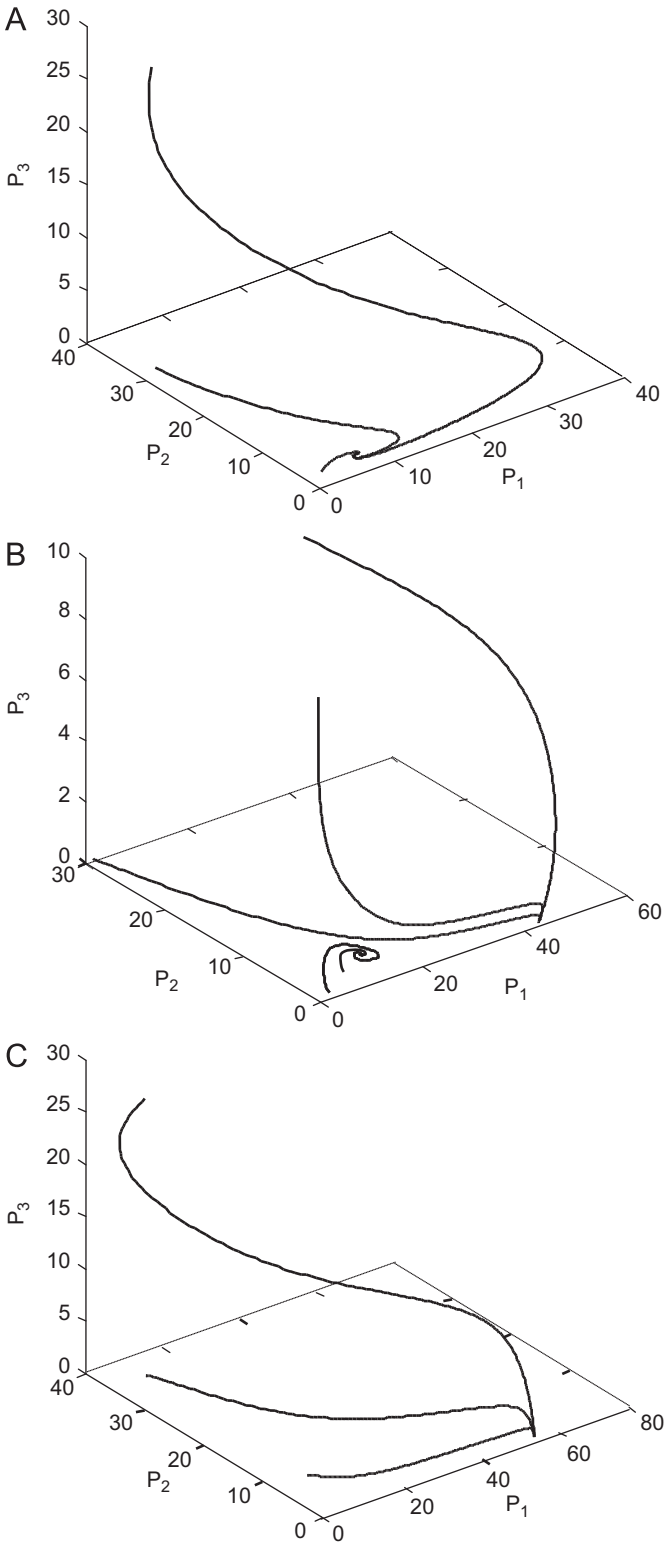

Fig. 3. Phase portraits of the model with food-mediated unsynchronized vertical migration (5) n=3, $r_i = r$, $\omega_i = \omega$, $\beta_i = \beta$. (A) Persistence of phytoplankton in a non-blooming regime (the stationary values of $P_i \ll K$ i=1,2,3) at low β (β=0.02). (B) Coexistence of two stable stationary states for intermediate values of β (β=0.06) implying bi-stability. The stationary state with $P_i \ll K$ is a non-blooming regime; the other state describes an algal bloom ($K \sim P_1 \gg P_{2,3}$). (C) For large values of β (β=0.08), the only possible stationary state is a blooming regime. The other system parameters are chosen as K=80; μ=0.8; γ=0.2; r=1.5.

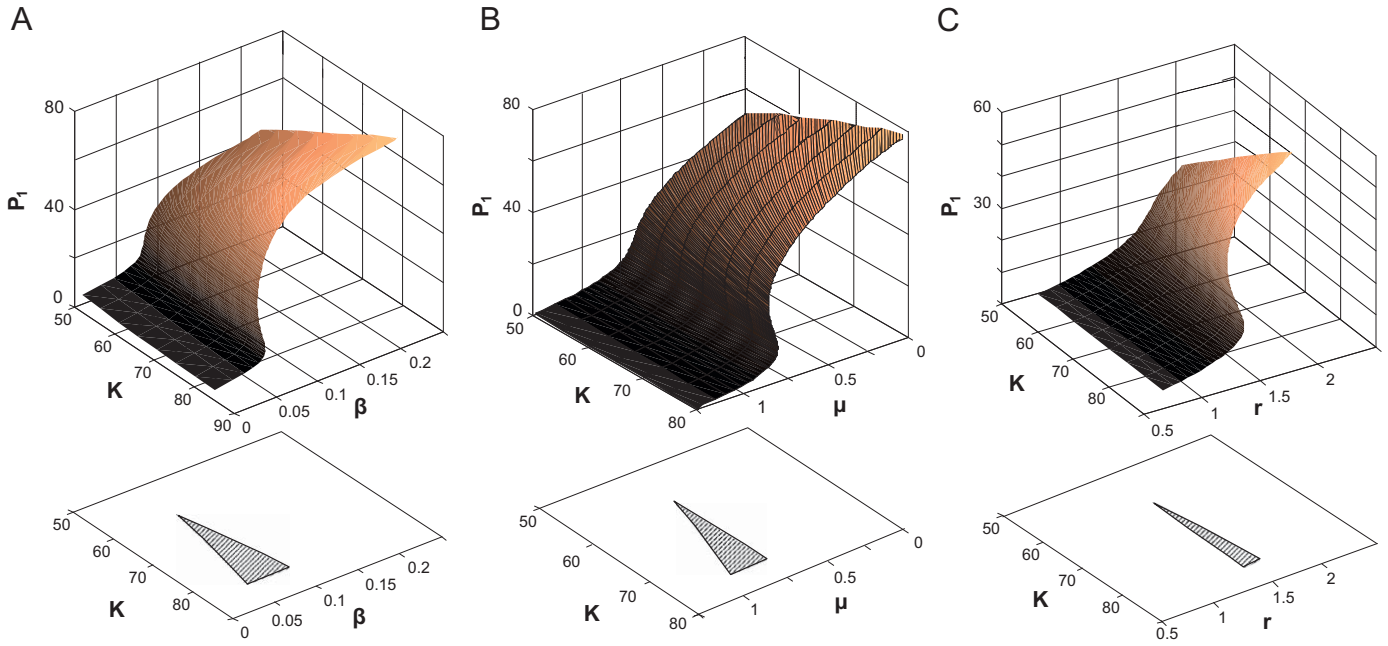

Fig. 4. Two-dimensional bifurcation diagrams of model (5) constructed for n=3 and $r_i = r$, $\omega_i = \omega$, $\beta_i = \beta$. In the upper row, the stationary stable density P_1 is shown depending on system parameters. In the lower row, the location of the bistability regions is shown (hatched domains). We used the following parameter values: (A) μ=0.8; γ=0.2; r=1.5; (B) β=0.02; μ=0.8; γ=0.2; r=1.5 and (C) β=0.02; μ=2.5; γ=0.2.

other one characterized by large algal density in the surface layer ($P_1 \gg P_{2,3}$). The latter can be interpreted as an algal boom. Finally, for large β (pronounced saturation in feeding of herbivorous) the only possible stable stationary state is a bloom stationary state (Fig. 3C). In other words, zooplankton cannot control the phytoplankton growth at low algal densities. Note that we have not found any other types of dynamics (i.e. regular or chaotic oscillations) for $r_i = r$, $\omega_i = \omega$, $\beta_i = \beta$.

To understand better the dependence of the system's behaviour on the parameters, we have constructed a large number of two-dimensional bifurcation diagrams. Some of them are represented in Fig. 4. In each diagrams, we show the stationary density of phytoplankton P_1 in the surface layer depending on system parameters. Note that in case $P_1 > 0$, this signifies that $P_{2,3} > 0$. In the lower row in Fig. 4, we show the locations of the bistability regions in the diagrams by hatching those regions. On the borders of those regions, a fold bifurcation occurs (see Kuznetsov, 1995). Note that for small values of K, a variation of a second parameter does not result in crossing the bistability region. In this case, to distinguish between a bloom from a non-bloom stationary state, we can use the following criterion for the bloom state: $P_1 > K/2$.

One can see from the diagrams that the control of phytoplankton by zooplankton (i.e. $P_1 \ll K/2$) becomes possible within a large range of system parameters and requires low values of β and r (high half-saturation density, low algal growth rates) and high values of μ (large amount of zooplankton in the system). Note that, although an increase in the carrying capacity K would result in the appearance of the 'bloom' stationary state, the grazing control phytoplankton at low algal densities is still possible even for very large values of K (formally, for $K \to \infty$, corresponding to highly eutrophic ecosystems). This is impossible for model (7) with the classical grazing term.

Let us consider briefly a more realistic situation, when the absorption of water is taken into account. This reduces the algal growth coefficients in lower layers and can be parameterised in the following way: $r_2 = r_1\lambda$, $r_3 = r_2\lambda$. The coefficient λ satisfies $0 < \lambda < 1$ (cf. Herman and Platt, 1983). We should say that by varying λ and considering realistic ranges of other system's parameters, we did not find any new type of system behaviour compared to the case with $\lambda = 1$. Simulations show that the domain in the parameter space, corresponding to the non-blooming stationary state shrinks with a decrease of λ. Fig. 5 illustrates such a decrease by providing 1-dimensional parametric portraits for different λ for low and high values of β. The influence of water absorption on the system's dynamics can be analysed based on (7) as well. The condition of persistence of phytoplankton now becomes $r_1 > 3\mu/(1+\lambda+\lambda^2)$. As such, one can see that absorption of light by water deteriorates conditions of phytoplankton persistence, however, for $r_1 > 3\mu$, persistence of phytoplankton would always takes place for any $0 < \lambda < 1$.

We analysed as well the situation when the local functional responses are different in different layers. This can arise due to a number of reasons: difference of hydrological conditions in the layers, temperature regimes, etc (Dam and Peterson, 1998). Since the number of system parameters becomes substantially larger in this case, we considered a scenario when the maximum grazing rates in the layers decrease with depth: $\omega_2 = \omega_1\lambda$, $\omega_3 = \omega_2\lambda$, where $0 < \lambda < 1$. The bifurcation diagrams are represented in Fig. 6 constructed for different λ. We use μ_1 as a bifurcation parameter, which is proportional to the total amount of zooplankton in the column. We found self-sustained oscillations for small values of λ. The maximum and minimum values of species densities during oscillations are shown by dotted lines. There might be also a situation when stable oscillations and stable equilibrium point coexist for the same set of parameters. Overall, we found that control algal growth, for small λ (i.e. for poor grazing conditions in lower layers) would require a larger total amount of zooplankton in the system than in case of identical functional responses. However, we should say that the situation with small λ ($\lambda < 0.5$) should be considered more as exotic since it suggests rather harsh feeding conditions in deep layers compared to the surface layer.

Finally, we investigated the behaviour of model (5) for different number of layers. In particular, the stability of the zero state and that of non-blooming stationary state was investigated

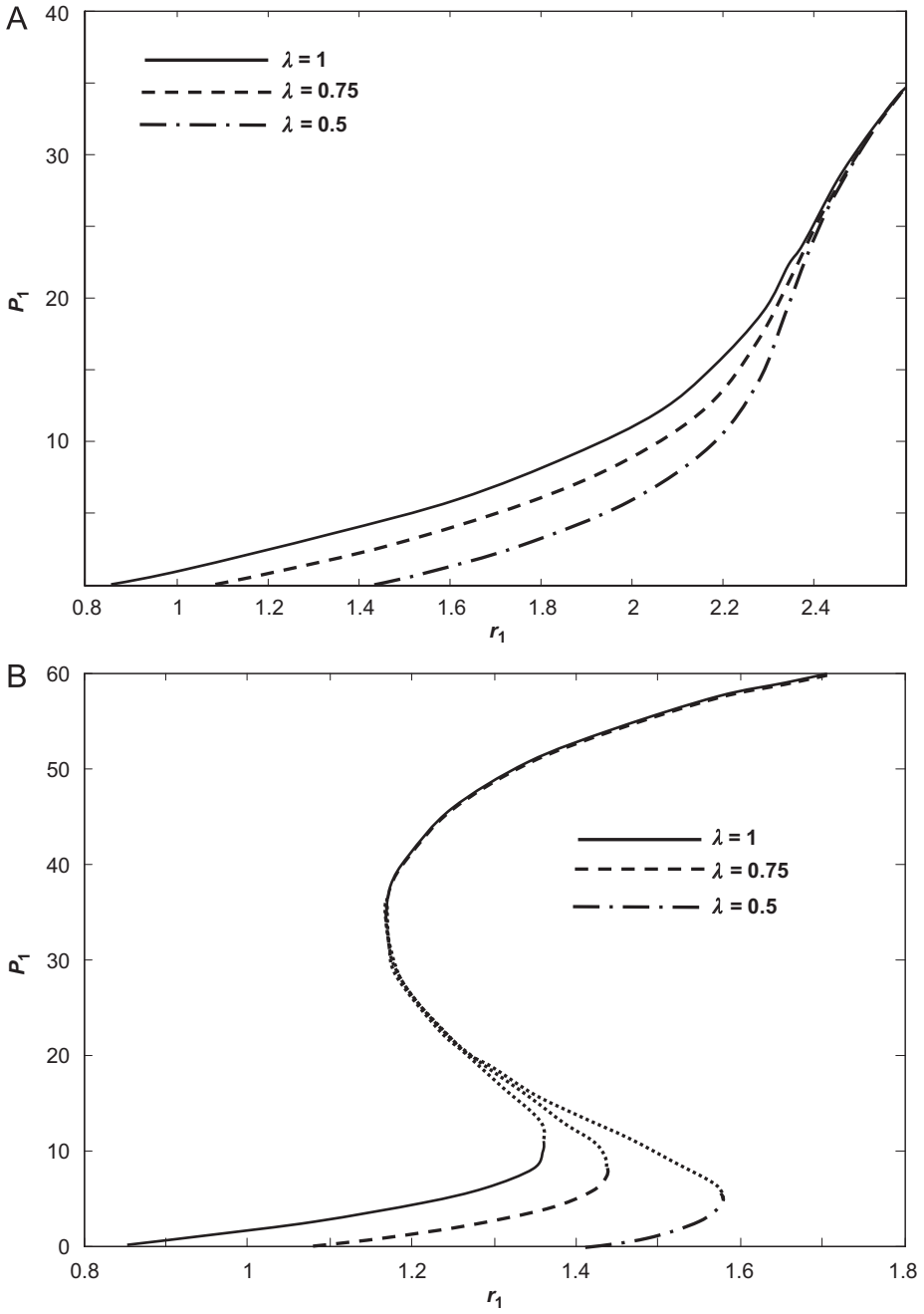

Fig. 5. Behavior of model (5) in case of strong absorption of light by water: $r_2 = r_1\lambda$, $r_3 = r_2\lambda$, $0 < \lambda < 1$. We show P_1 of the stationary stable state(s) depending on the growth rate r_1 in the upper layer. The unstable stationary state is denoted by dashed line. The diagrams A and B are constructed for low and high values of β (β=0.02 and 0.08, respectively). The other system parameters are K=80; μ=0.8; γ=0.2.

analytically for n=2 (see Appendices B, C). We should say that the results obtained for the number of layers n=3 remain similar for $n \neq 3$. In particular, persistence of algae in the water column takes place within a large range of realistic system parameters. Also, grazing control by zooplankton at low algal densities becomes possible for $K \to \infty$. The dependence of the model behaviour on bifurcation parameters for $n \neq 3$ is similar to the one shown in Figs 4–6. Note, however, that n cannot be too large in (5) since it would imply narrow layers and we will need to take into account the exchange of algae between the layers due to vertical turbulent diffusion.

5. Discussion

Feeding of zooplankton in the ocean (or deep lakes) implies existence of complex foraging cycles characterized by permanent exchange of grazers between surface and deep layers (Pearre, 1979; Leising et al., 2005; Cottier et al., 2006). In this paper, we provide an example of such unsynchronized vertical migration for herbivorous copepods based on our field data. We show as well that one should be extremely careful when assuming the rate of consumption of food by zooplankton to be equal to the product of the zooplankton density at a given depth and the local functional

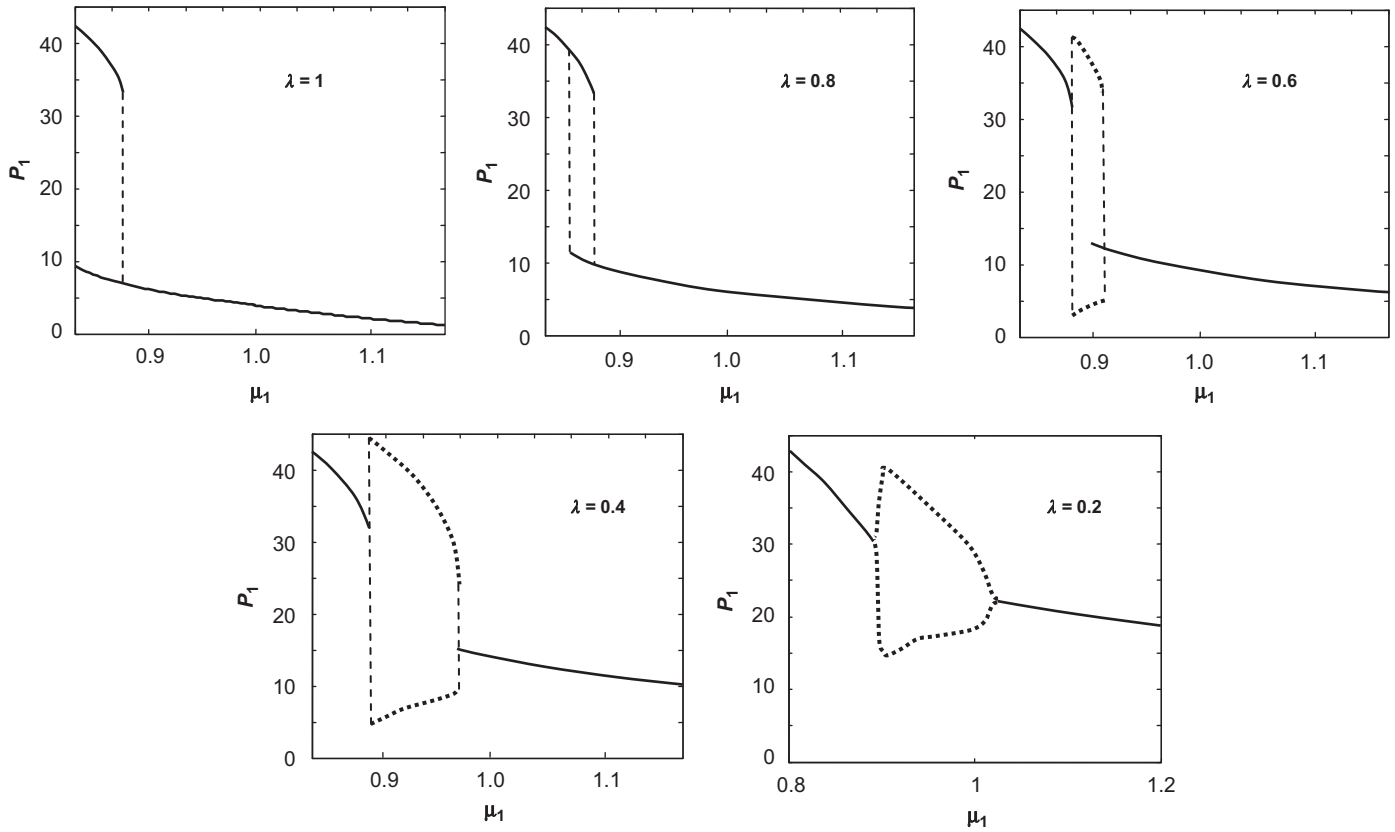

Fig. 6. Behavior of model (5) with different maximal consumption rates in local functional responses (4) in different layers, which is parameterized by $\omega_2=\omega_1\lambda$, $\omega_3=\omega_2\lambda$. By solid line we denote the stationary stable state(s); by dotted line we show the maximum and minimum values of P_1 during oscillations. The bifurcation parameter is $\mu_1=\omega_1 Z$ (Z is the average zooplankton density). The other system parameters are K=80; r=1.5; μ=0.8; γ=0.2.

response. The 'classical' local functional response, i.e. a function by which we need to multiply the ambient density of predator to compute the grazing rate in a layer, might simply not exist in ecosystems with a pronounced depth. As a consequence, plankton models should be amended somehow to provide an adequate description of reality.

In this paper, we suggested a simple way of incorporating effects of unsynchronized vertical migration into mean-field equations by taking into account the existence of two different phases of feeding cycle: consumption of food (active phase) and digestion (non-active phase). The actual grazing in each horizontal layer is determined by the density of actively feeding zooplankton and not by the total density Z_i of organisms in the layer. This can explain the usual failure to reveal local functional response *in situ*, when *all* organisms sampled at a given depth are used to estimate the feeding rate at this depth. We hypothesize that the partition of actively feeding organisms $\tilde{Z}_i$ among the layers depends on the vertical distribution of food. Food-mediated unsynchronized vertical migration enables dynamical adjustment of $\{\tilde{Z}_i\}$ to slow changing profile of phytoplankton $\{P_i\}$. Note that for our purpose we do not model explicitly evolution of the actual densities Z_i.

In our study, we compare two generic plankton models with explicit vertical space. The first model (given by (6)) is based on the classical approach of description of grazing. The second model (given by (5)) takes into account food-dependant distribution of active feeders in layers caused by unsynchronized migration. Our comparison of the behaviour of the two models suggests that taking into account food-mediated unsynchronized vertical migration would make a plankton model more realistic. Below, we summarize main advantages of the use of the new approach.

First, in the model with food-mediated unsynchronized vertical migration, persistence of species becomes greatly enhanced. Persistence of phytoplankton becomes possible within a wide range of system parameters. On the contrary, the classical model (6) predicts non-extinction of species for an extremely small parameter region (see Fig. 2). A slight variation of system parameters, caused by eventual environmental noise and/or oscillation of the zooplankton densities in layers, would result into extinction of phytoplankton in some layers. The classical model also predicts that persistence of algae should take place mostly due to avoidance of deep food-rich layers by zooplankton. Such scenario cannot be accepted as typical for real plankton communities.

We should admit that there can be some mechanisms amending persistence conditions in the classical model (6) as well. For instance, dynamical self-adjustment of the zooplankton densities Z_i would help avoid overgrazing. A particular example is the so called ideal free distribution (Giske et al., 1997; Lampert, 2005), when vertical distribution of zooplankton follows that of relative proportion of food in the water column. We should say, however, that the ideal free distribution (IFD) is not always supported by real field data. In particular, we did not find any evidence for an IFD in the ecosystem under study. This could be explained by the fact that one should look for the IFD of actively grazing organisms $\tilde{Z}_i$ and not that of total zooplankton Z_i. Another possibility to avoid overgrazing in (6) is taking into account changes in the total zooplankton biomass due to consumer-resource cycles. However, such a scenario would be rather doubtful on the considered short time scale (10 days) for large-sized copepods with the life cycle of 1–2 years (Melle and Skjoldal, 1998; Falk-Petersen et al., 1999). Moreover, noisy environment makes such regulation even less possible. On the contrary,

considering food-mediated non-synchronous vertical migration does not need implementation of the above assumptions and guarantees non-extinction of species within a large range of variation of total amount of zooplankton in the system (see Fig. 4).

Second, model with food mediated unsynchronized vertical migration shows enhancement of ecosystem's stability and suppression of algal blooms. Indeed, for a large range of system parameters, model (5) has a stable stationary state with low phytoplankton densities in all layers. In particular, a stable stationary state with $P_{1,2,3} \ll K$ is possible within large range of the parameters μ_i, which are proportional to total amount of zooplankton in the system. This signifies that phytoplankton growth can be successively controlled by zooplankton even in case of a large variation of the total amount of zooplankton in the column. This is rather new property compared to models with only local grazing. The mechanism of bloom regulation is similar to the emergence of a sigmoid overall functional response for the whole zooplankton population from non-sigmoid local responses (Morozov et al., 2008; Morozov and Arashkevich, 2008). It is well known that the sigmoid functional response enhances stability of resource-consumer systems (Oaten and Murdoch, 1975).

Third, a successful control of phytoplankton by zooplankton in model (5) is possible for very large values of carrying capacities (formally, for $K \to \infty$). On the contrary, the classical model exhibits in this case pathological behaviour, i.e. showing $P_1 \to \infty$, $P_{2,3} \to 0$ for all initial conditions and all values of parameters. As such, food-mediated unsynchronized vertical migration can be suggested as a possible solution of the paradox of enrichment in aquatic ecosystems (Rosenzweig, 1971; Gilpin, 1972; Jansen, 1995; Morozov et al., 2007). According to the paradox of enrichment, a gradual increase of the resource stock for prey (i.e. an increase of the carrying capacity) in a predator–prey system should destabilize the system when the functional response of the predator is of Holling type II. In real ecosystems, however, the predicted destabilization often does not take place. In model (5), where the local functional response is of Holling type II, food-mediated unsynchronized vertical migration results in selective feeding of zooplankton in layers with maximal concentration of food. In such system, the possibility of suppression of algal growth at low algal density is not affected by K, at least for small perturbations of the stable stationary state. This could model the 'paradoxical' behaviour real plankton ecosystems which often do not exhibit destabilization as a response to an increase of the nutrients' load on the system.

Note that the behaviour of model (1)–(2) would depend on the parameterization of the consumption vector $A=\{\alpha_i\}$. For instance, model (1)–(2) with constant coefficients α_i, will be equivalent to the classical model (6). As such, an important condition to obtain enhancement of stability is that the proportion of active grazers in a given layer should increase with an increase of relative proportion of food this layer, as suggested in (4).

We should say that an accurate parameterization of α_i, is rather a challenging issue since it would require the use of radioactive tracers to follow vertical displacement of organisms during a foraging cycle. For instance, it was virtually impossible, based on our own data on feeding of *Calanus* spp. *in situ*, to reveal a precise functional form of α_i. The major difficulty was that we could not identify precisely which individuals were in the active phase of their foraging cycle and which ones where digesting food at the moment of collection by nets. However, there is some evidence that the major grazing is being displaced mainly to layers with high food abundance, while the relative proportion of food in those layers is being increased. Our data reveal that the difference between ingestion rates in surface and deep layers becomes less pronounced with an increase of relative proportion of food in surface layers. In other words, the main consumption takes place in food rich layers and zooplankton almost do not consume food in deep layers. This signifies that the coefficients α_i would increase with an increase of proportion of food in layers and gives us certain background to the use of parameterization (3).

Note that in this paper we considered a rather generic plankton model, by neglecting some other factors which could influence the system's behaviour. This includes, for example, depletion of nutrients in the surface layers, exchange of phytoplankton among the horizontal layers due to random diffusion or due to altering the buoyancy of algae (Raymont, 1980), etc. Moreover, the total biomass of zooplankton in the water column may also change as a result of resource-consumer phyto-zooplankton cycles (e.g. Ryabchenko et al., 1997; Edwards and Brindley, 1999), which would result in oscillations of μ_i. Our preliminary analysis, however, shows that in the latter case, variation of μ_i due to consumer-resource cycles would make the system even more stable. We are planning to address the mentioned issues in our next paper.

Acknowledgements

We highly appreciated S.V. Petrovskii (University of Leicester) for a careful reading and comments. We would like to thank C. Halsband-Lenk (Plymouth Marine Laboratory) for stimulating discussions.

Appendix A

Here we consider stability properties of model (5). For the sake of simplicity we assume the number of layers $n=3$. Note, however, the analytical results can be easily extended to an arbitrary number of layers n. The system's equations are given by

$$\frac{dP_1}{dt} = r_1 P_1 \left(1 - \frac{P_1}{K}\right) - \mu_1 \frac{P_1}{1+\beta_1 P_1}, \tag{A1}$$

$$\frac{dP_2}{dt} = r_2 P_2 \exp(-\gamma_0 P_1)\left(1 - \frac{P_2}{K}\right) - \mu_2 \frac{P_2}{1+\beta_2 P_2}, \tag{A2}$$

$$\frac{dP_3}{dt} = r_3 P_3 \exp(-\gamma_0 (P_1+P_2))\left(1 - \frac{P_3}{K}\right) - \mu_3 \frac{P_3}{1+\beta_3 P_3}. \tag{A3}$$

The coordinates of non-trivial stationary states (i.e. $P_i \neq 0$, $i=1$, n) are defined by

$$0 = r_1 \left(1 - \frac{P_1}{K}\right) - \mu_1 \frac{1}{1+\beta_1 P_1}, \tag{A4}$$

$$0 = r_2 \exp(-\gamma_0 P_1)\left(1 - \frac{P_2}{K}\right) - \mu_2 \frac{1}{1+\beta_2 P_2}, \tag{A5}$$

$$0 = r_3 \exp(-\gamma_0 (P_1+P_2))\left(1 - \frac{P_3}{K}\right) - \mu_3 \frac{1}{1+\beta_3 P_3}. \tag{A6}$$

The stability properties of the stationary states (in case they exist) can be analysed with the help of the Jacobian matrix of the system, computed at stationary states. Note that the Jacobian matrix for an arbitrary n is low triangular, since the first equation depends only on P_1, the second depends only on P_1 and P_2, etc. As such, we can analyse the stationary states of first i equations not taking into account the equations for the lower layers. We start with Eq. (A1). Simple computation shows that (A4) has only one positive real solution if and only if

$$\mu_1 - r_1 < 0. \tag{A7}$$

Alternatively, (A4) has two real (positive) solutions if and only if

$$1 - K\beta_1 > 0 \quad \text{and} \quad r_1(K\beta_1+1)^2 - 4K\beta_1\mu_1 > 0. \tag{A8}$$

Assume that (A4) has one root, i.e. (A7) holds. This signifies the existence of a unique non-trivial stationary state of (A1). Simple analysis of this one-dimensional equation shows that this state is stable and the trivial stationary state $P_1=0$ is unstable. When (A4) has two real positive roots (see (A8)), the lower stationary state is unstable; the upper stationary state is stable. In this case, the trivial stationary state of becomes stable (i.e. a bistability takes place).

We add then Eq. (A2) to Eq. (A1). The conditions of existence of non-trivial stable stationary state(s) with $P_2 \neq 0$ can be computed in a similar way, as before. One can consider Eq. (A2) to be one-dimensional with the value of P_1 as a parameter (we require P_1 to be a non-trivial stable stationary state of (A1)). Thus, (A5) will have only one root if and only if

$$\mu_2 - r_2 \exp(-\gamma_0 P_1) < 0. \tag{A9}$$

Alternatively, (A5) has two roots if and only if

$$1 - K\beta_2 > 0 \quad \text{and} \quad r_2(K\beta_2+1)^2 \exp(-\gamma_0 P_1) - 4K\beta_2\mu_2 > 0. \tag{A10}$$

In case (A9) holds, system (A1)–(A2) has a unique non-trivial stable stationary state (P_1, P_2). The trivial stationary state (P_1, 0) is unstable. When (A10) is satisfied, (A5) has two real positive roots. The one with larger P_2 is stable. It will provide a stable stationary state for (A1)–(A2). Note that the trivial stationary state (P_1, 0) is stable as well.

In a similar way, one can add (A3) into (A1)–(A2) and analyse the existence of and stability of three-dimensional non-trivial stationary states. This gives the following conditions of existence of the non-trivial stationary stable state (P_1, P_2, P_3) for (A1)–(A3):

$$\mu_3 - r_3 \exp(-\gamma_0 P_1 - \gamma_0 P_2) < 0, \tag{A11}$$

or, alternatively,

$$1 - K\beta_3 > 0 \quad \text{and} \quad r_3(K\beta_3+1)^2 \exp(-\gamma_0 P_1 - \gamma_0 P_2) - 4K\beta_3\mu_3 > 0, \tag{A12}$$

where P_1, P_2 are non-trivial stationary stable states for (A1)–(A2).

Remark. It is easy to prove that the only attractors of the system with local grazing terms are stationary states (periodic or/chaotic oscillations cannot exist). This follows from the fact there can be no oscillations in (A1), thus P_1 will approach a stable stationary state. The same concerns (A2), since after some $t>0$, P_1 can be considered as a parameter close to its stationary value.

Appendix B

Here we analyse stability properties of the zero stationary state of model (5). We consider the number of layers $n=3$ (we briefly address the case $n=2$ at the end). In the vicinity of (0,0,0) the system equations become

$$\frac{dP_i}{dt} = r_i P_i - \overline{\mu}_i \frac{P_i^2}{P_0}, \tag{B1}$$

where $P_0 = P_1+P_2+P_3$, where $\overline{\mu}_i = 3\mu_i$, $i=1, 2, 3$. From (B1) one can easily derive that a necessary condition of stability is $r_i - \overline{\mu}_i < 0$, otherwise the right-hand side functions are always positive and a small perturbation of the stationary state will always increase.

Note that the right-hand side functions are discontinuous at zero. However, by replacing time by $P_0\, d\tau = dt$, system (B1) can be re-written in the following way:

$$\frac{dP_i}{d\tau} = (r_i P_0 - \overline{\mu}_i P_i) P_i. \tag{B2}$$

Note that Eq. (B2) cannot be linearized in the vicinity of zero and the standard linear stability analysis method is not applicable. A possible way to investigate the behaviour in the vicinity of (0,0,0) can be a suitable change of variables. This method is often implemented in stability analysis of planar systems with de-generated stationary states (e.g. Berezovskaya et al., 2001). However, in case the dimension of the system $n=3$, such an approach becomes rather cumbersome. Here we use another method based on graphical representation of the phase portraits. We construct the surfaces with $\dot{P}_i = 0$. They are given by the following equations of planes:

$$(r_1 - \overline{\mu}_1)P_1 + r_1 P_2 + r_1 P_3 = 0 \;\Rightarrow\; \dot{P}_1 = 0, \tag{B3}$$

$$r_2 P_1 + (r_2 - \overline{\mu}_2)P_2 + r_2 P_3 = 0 \;\Rightarrow\; \dot{P}_2 = 0, \tag{B4}$$

$$r_3 P_1 + r_3 P_2 + (r_3 - \overline{\mu}_3)P_3 = 0 \;\Rightarrow\; \dot{P}_3 = 0. \tag{B5}$$

The planes (B3)–(B5) divide the positive octant into regions with a constant sign of $\dot{P}_i$. By considering different combinations of mutual positions of (B3)–(B5), we found that stability of the zero state takes places only in the case shown in Fig. B1.A. By arrows, we show schematically the direction of the differential flow given by (B2). This helps follow behaviour of system's trajectories. In the vicinity of (0,0,0), any system trajectory enters the pyramid which is formed by intersection of the three planes in the positive octant. Further, the trajectory will approach zero inside the pyramid. Note that all other combinations of mutual arrangement of planes (B3)–(B5) will make any trajectory to leave the vicinity of (0,0,0), i.e. this point will be a repeller. An example of such situation is shown in Fig. B1.B. We do not show here other combinations of mutual positions of (B3)–(B5) with unstable behaviour for the sake of brevity.

Fig. B1.A. allows to derive the stability criterion (7). To have the mutual arrangement of (B3)–(B5) as it is shown in the figure, the necessary and sufficient conditions are the following:

(i) intersection of $\dot{P}_1 = 0$ and $P_2 = 0$ should lie higher than the intersection of $\dot{P}_3 = 0$ and $P_2 = 0$;
(ii) the normal vector $\underline{k}$ of the plane $\dot{P}_2 = 0$ (having a negative z-coordinate) and the vector $\underline{l}$, parallel to the line of intersection of $\dot{P}_1 = 0$ and $\dot{P}_3 = 0$ (having a positive z-coordinate) should form an acute angle.

The first condition gives us $r_3\overline{\mu}_1 + \overline{\mu}_3 r_1 - \overline{\mu}_1\overline{\mu}_3 < 0$.

To find the analytical expression for the second condition we need to compute $\underline{l}$. After some analytical work we get

$$\underline{l} = \left(\frac{-\overline{\mu}_3 r_1}{r_3\overline{\mu}_1 + \overline{\mu}_3 r_1 - \overline{\mu}_1\overline{\mu}_3}, 1, \frac{-\overline{\mu}_1 r_3}{r_3\overline{\mu}_1 + \overline{\mu}_3 r_1 - \overline{\mu}_1\overline{\mu}_3} \right).$$

The normal vector $\underline{k}$ of (B4) is given by: $\underline{k} = (-r_2, \overline{\mu}_2, -r_2, -r_2)$. Thus, the condition (ii) becomes $\underline{k} \cdot \underline{l} > 0$. Finally, after some simplification this condition can be re-written as

$$\frac{r_1\overline{\mu}_2\overline{\mu}_3 + r_2\overline{\mu}_1\overline{\mu}_3 + r_3\overline{\mu}_1\overline{\mu}_2 - \overline{\mu}_1\overline{\mu}_2\overline{\mu}_3}{r_3\overline{\mu}_1 + \overline{\mu}_3 r_1 - \overline{\mu}_1\overline{\mu}_3} > 0.$$

Note that the above condition can be re-written in a more compact form (returning to μ_i):

$$r_1\mu_2\mu_3 + r_2\mu_1\mu_3 + r_3\mu_1\mu_2 - 3\mu_1\mu_2\mu_3 < 0. \tag{B6}$$

Inequality (B7) automatically includes both conditions (i) and (ii) and provides the necessary and sufficient condition of (local) stability of the zero point (0,0,0).

Remark. By implementing the same graphical method as in $n=3$, it is easy to show that the stability of the zero stationary state of system (5) for $n=2$ is possible if and only if:

$$r_1\mu_2 + r_2\mu_1 - 2\mu_1\mu_2 < 0. \tag{B7}$$

In this case the curves with $\dot{P}_i = 0$ will be straight lines.

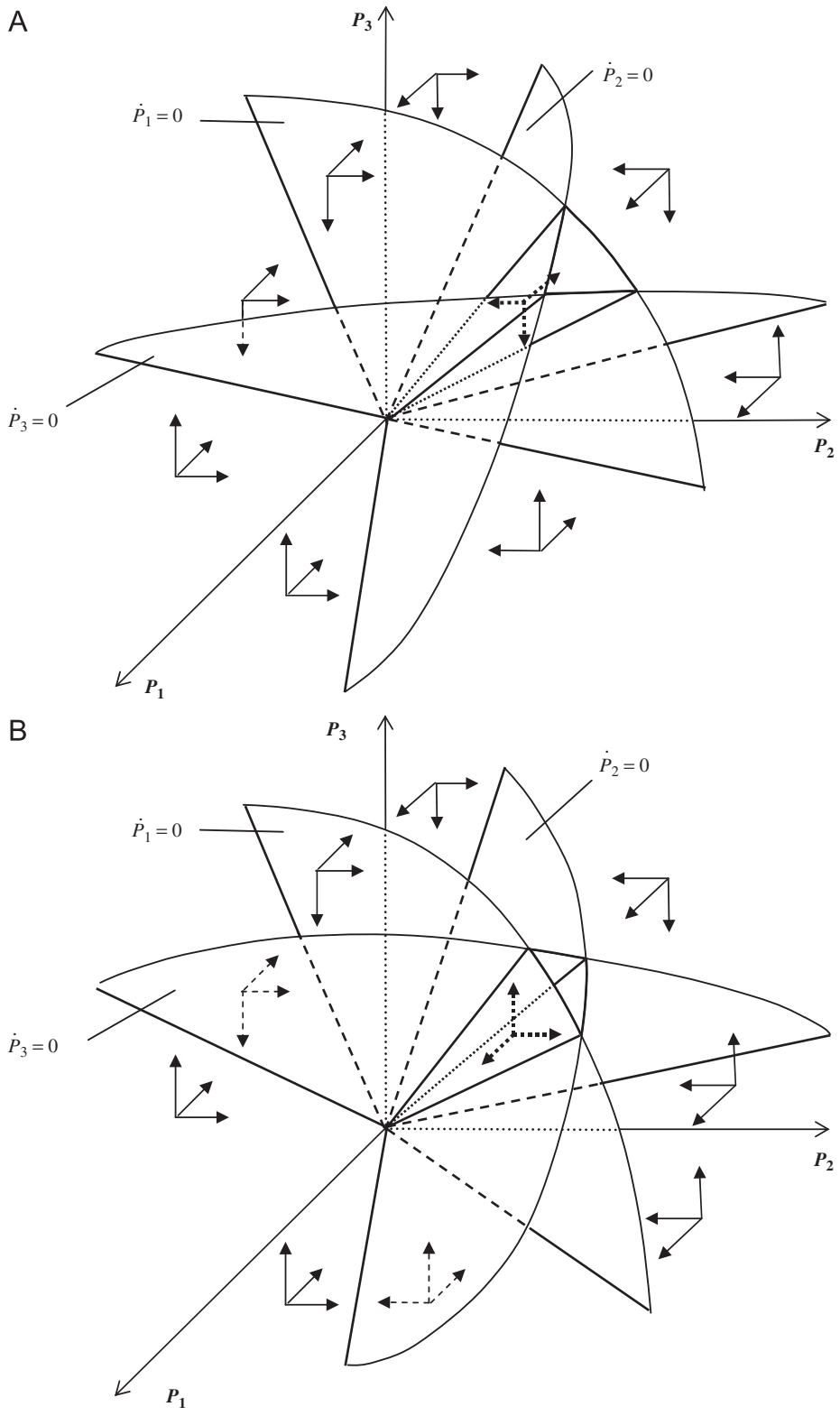

Fig. B1

Appendix C

Here we analyse stability properties of the non-blooming stationary state of model (5), i.e. the one with $0 < P_i \ll K$, for the number of layers $n=2,3$. First, we consider $n=2$. The stationary densities of species can be found from the following equations:

$$0 = r_1\left(1 - \frac{P_1}{K}\right) - \overline{\mu}_1 \frac{1}{1+\beta_1 P_1}\frac{P_1}{P_0}, \tag{C1}$$

$$0 = r_2 \exp(-\gamma_0 P_1)\left(1 - \frac{P_2}{K}\right) - \overline{\mu}_2 \frac{1}{1+\beta_2 P_2}\frac{P_2}{P_0}, \tag{C2}$$

where $P_0 = P_1 + P_2$, $\overline{\mu}_i = 2\mu_i$. Eqs. (C1)–(C2) cannot be solved analytically. Let us consider the case when the half-saturation rates is high ($1/\beta \gg 1$); moreover, for a non-blooming state we have $P_i \ll K$. This gives us simpler equations for the stationary state:

$$0 = r_1 - \overline{\mu}_1 \frac{P_1}{P_1 + P_2}, \tag{C3}$$

$$0 = r_2 \exp(-\gamma_0 P_1) - \overline{\mu}_2 \frac{P_2}{P_1 + P_2}. \tag{C4}$$

As in Appendix B, we consider that $r_i - \overline{\mu}_i < 0$. The stationary density P_1 in the upper layer is determined by the following equation:

$$r_2 \exp(-\gamma_0 P_1) = \overline{\mu}_2 \frac{(\overline{\mu}_1 - r_1)}{\overline{\mu}_1}. \tag{C5}$$

Simple computing gives the stationary densities of species

$$P_1 = -\frac{1}{\gamma_0} \ln\left[\frac{\overline{\mu}_2}{\overline{\mu}_1}\frac{(\overline{\mu}_1 - r_1)}{r_2}\right]; P_2 = \frac{(\overline{\mu}_1 - r_1)}{r_1} P_2. \tag{C6}$$

From (C6) one can see that the non-blooming stationary state exists only in case ($\overline{\mu}_i = 2\mu_i$):

$$r_1\mu_2 + r_2\mu_1 - 2\mu_1\mu_2 > 0. \tag{C7}$$

By comparing (C7) with condition (B7) from Appendix B one can conclude that the loss of stability of the zero stationary state (when a bifurcation parameter is being varied) occurs via a birth of a stationary state (C6) in the vicinity of zero. Stability of this stationary state can be determined via the standard linear analysis method. The trace of the matrix of the linearized system at the stationary state becomes

$$SpA = -r_1 + \frac{r_1^2}{\overline{\mu}_1} - r_2 \exp(-\gamma_0 P_1) + \frac{r_2^2}{\overline{\mu}_2} \exp(-2\gamma_0 P_1). \tag{C8}$$

After having plugged (C6) into (C8), we obtain the following condition of stability:

$$\overline{\mu}_1 - r_1 > 0 \quad \text{or} \quad 2\mu_1 - r_1 > 0. \tag{C9}$$

This is a necessary condition of existence of non-blooming stationary state. This signifies that the stationary state is always stable. Thus, the loss of stability of the trivial stationary state (0,0) takes place via a birth of *stable* stationary state in the vicinity of (0,0).

Let us investigate now the stability of the non-blooming stationary state when the number of layers $n=3$. As before, we consider that $r_i - \overline{\mu}_i < 0$. The stationary densities of species are determined by

$$0 = r_1 - \overline{\mu}_1 \frac{P_1}{P_0}, \tag{C10}$$

$$0 = r_2 \exp(-\gamma_0 P_1) - \overline{\mu}_2 \frac{P_2}{P_0}, \tag{C11}$$

$$0 = r_3 \exp(-\gamma_0 P_1 - \gamma_0 P_2) - \overline{\mu}_3 \frac{P_2}{P_0}, \tag{C12}$$

where $P_0 = P_1 + P_2 + P_3$, $\overline{\mu}_i = 3\mu_i$.

A rather straightforward computing provides the equation for the stationary density P_1 in the surface layer:

$$r_3 \exp\left(-\gamma_0 P_1 \frac{\overline{\mu}_2 + r_2\mu_1 \exp(-P_1\gamma_0)}{\overline{\mu}_2}\right)\overline{\mu}_1\overline{\mu}_2 + \overline{\mu}_2\overline{\mu}_3 r_1 + \overline{\mu}_1\overline{\mu}_2 r_2 \exp(-\gamma_0 P_1) - \overline{\mu}_1\overline{\mu}_2\overline{\mu}_3 = 0. \tag{C13}$$

This is a transcendental equation and it cannot be solved analytically. Let us suppose that P_1 is small. In this case we can neglect the exponential function in the exponential term. We obtain

$$\exp(-\gamma_0 P_1) = \frac{1}{r_3}\frac{\overline{\mu}_2\overline{\mu}_3(\overline{\mu}_1 - r_1)}{\overline{\mu}_1\overline{\mu}_2 r_3 + \overline{\mu}_1\overline{\mu}_2 r_2}. \tag{C14}$$

The other stationary densities can be easily computed from

$$P_2 = \frac{r_2\overline{\mu}_1}{r_1\overline{\mu}_2} P_1 \exp(-\gamma_0 P_1), \quad P_3 = \frac{r_2\overline{\mu}_1(\overline{\mu}_1 P_1 - r_1 P_1 - r_1 P_2)}{r_1}. \tag{C15}$$

Thus, to have positive P_i, $i=1, 2, 3$, the following conditions should be satisfied:

$$r_1\overline{\mu}_2\overline{\mu}_3 + r_2\overline{\mu}_1\overline{\mu}_3 + r_3\overline{\mu}_1\overline{\mu}_2 - \overline{\mu}_1\overline{\mu}_2\overline{\mu}_3 > 0.$$

Coming back to μ_i we obtain

$$r_1\mu_2\mu_3 + r_2\mu_1\mu_3 + r_3\mu_1\mu_2 - 3\mu_1\mu_2\mu_3 < 0. \tag{C16}$$

One can see from (C16) that the first condition is the opposite to the condition of stability of the zero stationary state given by (B6). In other words, the loss of stability of the state (0,0,0) occurs via a birth of non-trivial stationary state in the vicinity of zero. The stability of this state can be analysed via a standard linear analysis approach. By implementing the ***Routh–Hurwitz*** stability criterion, it is possible to show that the non-blooming stationary state with $P_i \ll 1$ is stable. However, we should say that the proof leads to rather cumbersome analytical expressions and we do not show them here. Thus, the loss of stability of the trivial stationary state, take place via a birth of *stable* stationary state.

References

Batchelder, H.P., Edwards, C.A., Powell, T.M., 2002. Individual-based models of zooplankton populations in coastal upwelling regions: implications of diel vertical migration on emographic success and nearshore retention. Prog. Oceanogr. 53, 307–333.

Berezovskaya, F., Karev, G., Arditi, R., 2001. Parametric analysis of the ratio-dependent predator–prey model. J. Math. Biol. 43, 221–246.

Bollens, S.M., Frost, B.W., 1989. Predator induced diel vertical migration in a marine planktonic copepod. J. Plankton Res. 11, 1047–1065.

Boyd, C.M., Smith, S.M., Cowles, T., 1980. Grazing patterns of copepods in the upwelling system off Peru. Limnol. Oceanogr. 25, 583–596.

Carlotti, F., Wolf, K.U., 1998. A Lagrangian ensemble model of *Calanus finmarchicus* coupled with a 1-D ecosystem model. Fish. Oceanogr. 7, 191–204.

Cottier, F.R., Tarling, G.A., Wold, A., Falk-Petersen, S., 2006. Unsynchronised and synchronised vertical migration of zooplankton in a high Arctic fjord. Limnol. Oceanogr. 51, 2586–2599.

Dagg, M.J., Wyman, K.D., 1983. Natural ingestion rates of the copepods *Neocalanus plumchrus* and *N. cristatus* calculated from gut contents. Mar. Ecol. Prog. Ser. 13, 37–46.

Dagg, M.J., Walser, W.E., 1987. Ingestion, gut passage, and egestion by the copepod *Neocalanus plumchrus* in the laboratory and in the subarctic Pacific Ocean. Limnol. Oceanogr. 32, 178–188.

Daase, M., Eiane, K., Aksnes, D.L., Vogedes, D., 2008. Vertical distribution of Calanus spp. and Metridia longa at four Arctic locations. Mar. Biol. Res. 4, 193–207.

Dam, H.G., Peterson, W.T., 1998. The effect of temperature on the gut clearance rate constant of planktonic copepods. J. Exp. Mar. Biol. Ecol. 123, 1–14.

DeMott, W.R., 1982. Feeding selectivities and relative ingestion rates of Daphnia and Bosmina. Limnol. Oceanogr. 27, 518–527.

Edwards, A.M., Brindley, J., 1999. Zooplankton mortality and the dynamical behavior of plankton population models. Bull. Math. Biol. 61, 202–339.

Falk-Petersen, S., Pedersen, G., Kwasniewski, S., Hegseth, E.N., Hop, H., 1999. Spatial distribution and life-cycle timing of zooplankton in the marginal ice zone of the Barents Sea during the summer melt season in 1995. J. Plankton Res. 21, 1249–1264.

Fossheim, M., Primicerio, R., 2008. Habitat choice by marine zooplankton in a high-latitude ecosystem. Mar. Ecol. Prog. Ser. 364, 47–56.

Franks, P., 2001. Phytoplankton blooms in a fluctuating environment: the roles of plankton response time scales and grazing. J. Plankton Res. 23, 1433–1441.

Gentleman, W., Leising, A., Frost, B., Storm, S., Murray, J., 2003. Functional responses for zooplankton feeding on multiple resources: a review of assumptions and biological dynamics. Deep-Sea Res. II 50, 2847–2875.

Gilpin, M.E., 1972. Enriched predator–prey systems: theoretical stability. Science 177, 902–904.

Giske, J., Rosland, R., Berntsen, J., Fiksen, O., 1997. Ideal free distribution of copepods under predation risk. Ecol. Mod. 95, 45–59.

Han, B.P., Straskraba, M., 1998. Modeling patterns of zooplankton diel vertical migration. J. Plankton Res. 20, 1463–1487.

Hansen, B., Tande, K.S., Berggreen, U.C., 1990. On the trophic fate of Phaeocystis pouchetii (Hariot). III. Functional responses in grazing demonstrated on juvenile stages of *Calanus finmarchicus* (Copepoda) fed diatoms and Phaeocystis. J. Plankton Res. 12, 1173–1187.

Herman, A.W., Platt, T., 1983. Numerical modelling of diel carbon production and zooplankton grazing on the Scotian shelf based on observational data. Ecol. Mod. 18, 55–72.

Holling, C.S., 1959. The components of predation as revealed by a study of small mammal predation of the European pine sawfly. Canad. Entomol. 91, 293–320.
Iwasa, Y., 1982. Vertical migration of zooplankton: a game between predator and prey. Am. Nat. 120, 171–180.
Jansen, V., 1995. Regulation of predator–prey systems through spatial interactions: a possible solution to the paradox of enrichment. Oikos 74, 384–390.
Jeschke, J.M., Kopp, M., Tollrian, R., 2002. Predator functional responses: discriminating between handling and digesting prey. Ecol. Monogr. 72, 95–112.
Kuznetsov, Y.A., 1995. Elements of Applied Bifurcation Theory. Springer, New York.
Lampert, W., 1992. Zooplankton vertical migrations: implications for phytoplankton–zooplankton interactions. Arch. Hydrobiol. Beih. Ergeb. Limnol. 35, 69–78.
Lampert, W., 2005. Vertical distribution of zooplankton: density dependence and evidence for an ideal free distribution with costs. BMC Biology 3, 10 (electronic).
Leising, A.W., 2001. Copepod foraging in patchy habitats and thin layers using a 2-D individual based model. Mar. Ecol. Prog. Ser. 216, 167–179.
Leising, A.W., Pierson, J.J., Cary, S., Frost, B.W., 2005. Copepod foraging and predation risk within the surface layer during night-time feeding forays. J. Plankton Res. 27, 987–1001.
Malkiel, E., Sheng, J., Katz, J., Strickler, J.R., 2003. The three-dimensional flow field generated by a feeding calanoid copepod measured using digital holography. J. Exp. Biol. 206, 3657–3666.
Melle, W., Skjoldal, H.R., 1998. Reproduction and development of *Calanus finmarchicus*, *C. glacialis* and *C. hyperboreus* in the Barents Sea. Mar. Ecol. Prog. Ser. 169, 211–228.
McLaren, J.A., 1963. Effect of temperature on growth of zooplankton and the adaptive value of vertical migration. J. Fish. Res. Board Can. 20, 685–727.
Morozov, A.Y., Arashkevich, E., 2008. Patterns of zooplankton functional response in communities with vertical heterogeneity: a model study. Math. Model. Nat. Phen. 3, 131–148.
Morozov, A.Y., Arashkevich, E., Reigstad, M., Falk-Petersen, S., 2008. Influence of spatial heterogeneity on the type of zooplankton functional response: a study based on field observations. Deep-Sea Res. II 55, 2285–2291.
Morozov, A.Y., Petrovskii, S.V., Nezlin, N.P., 2007. Towards resolving the paradox of enrichment in plankton community: role of zooplankton vertical migration. J. Theor. Biol. 248, 501–511.
Oaten, A., Murdoch, W.W., 1975. Functional response and stability in predator–prey systems. Am. Nat. 109, 289–298.
Ohman, M.D., 1990. The demographic benefits of diel vertical migration by zooplankton. Ecol. Monogr. 60, 257–281.
Pearre, S.J., 1979. Problems of detection and interpretation of vertical migration. J. Plankton Res. 1, 29–44.
Raymont, J.E.G., 1980. Plankton and Productivity in the Oceans. Phytoplankton. Pergamon, Oxford.
Rosenzweig, M.L., 1971. Paradox of enrichment: destabilization of exploitation ecosystems in ecological time. Science 171, 385–387.
Ryabchenko, V.A., Fasham, M.J.R., Kagan, B.A., Popova, E.E., 1997. What causes short-term oscillations in ecosystem models of the ocean mixed layer?. J. Mar. Syst. 13, 33–50.
Tande, K.S., Båmstedt, U., 1985. Grazing rates of the copepods *Calanus glacialis* and *C. finmarchicus* in arctic waters of the Barents Sea. Mar. Biol. 87, 251–258.
Tiselius, P., Jonsson, P.R., 1990. Foraging behaviour of six calanoid copepods: observations and hydrodynamic analysis. Mar. Ecol. Prog. Ser. 66, 23–33.
Tseng, L.-C., Kumar, R., Dahms, H.-U., Chen, Q.-C., Hwang, J.-S., 2008. Copepod gut contents, ingestion rates, and feeding impacts in relation to their size structure in the Southeastern Taiwan Strait. Zool. Stud. 47, 402–416.